Int. J. Heat Mass Transfer. Vol. 17, pp. 1391–1402. Pergamon Press 1974. Printed in Great Britain

THE GRAETZ PROBLEM WITH AXIAL HEAT CONDUCTION

M. L. MICHELSEN and JOHN VILLADSEN
Instituttet for Kemiteknik, Danmarks tekniske Højskole, 2800 Lyngby, Denmark

(*Received* 7 *December* 1973 *and in revised form* 21 *February* 1974)

Abstract—Using the Graetz problem with axial conduction as an illustrative example a method for solution of an important class of linear partial differential equations is developed. The method is a combination of orthogonal collocation and matrix diagonalization. The reason for the very high accuracy, which is obtained by collocation, is discussed in terms of the eigenvalues of the collocation operator. These are found to increase much faster than the true eigenvalues for $k > N/2$ where N is the number of collocation points, and this permits a high accuracy also in the "penetration region" of the solution where Fourier Series are slowly convergent.

Explicit formulas for the asymptotic Nu-number for large and small Pe-numbers are developed in an appendix. They are based on a perturbation of the eigenfunctions of the simplified model with either infinite or zero Pe-number.

A number of variants of the Graetz problem, which can be solved by a repetition of the present computations, are proposed.

NOMENCLATURE

- $\mathbf{A}$, discretization matrix for $\partial/\partial x$;
- $\mathbf{B}$, discretization matrix for $\partial^2/\partial x^2$;
- c_p, heat capacity of fluid;
- F_k, eigenfunction;
- J, dimensionless heat flux, equation (7);
- k, thermal conductivity of fluid;
- N, approximation order;
- Nu, Nusselt number, equation (6);
- Pe, Peclet number, equation (2);
- $\mathbf{Q}$, system matrix, equation (10);
- r, radial distance;
- R, tube radius;
- $\mathbf{S}$, matrix of eigenvectors, equation (11);
- T, fluid temperature;
- T_b, fluid temperature at $z \to -\infty$;
- T_0, wall temperature at $z \geqslant 0$;
- u, $(r/R)^2$;
- $\mathbf{U}$, discretization matrix for u;
- v_z, fluid velocity;
- $\langle v_z \rangle$, area mean fluid velocity;
- $\mathbf{V}$, discretization matrix for v_z;
- x, dimensionless radial distance, equation (1);
- y, dimensionless axial distance, equation (1);
- z, axial distance.

Greek symbols

- $\theta, \boldsymbol{\theta}$, dimensionless temperature, equation (1);
- $\bar{\theta}$, dimensionless bulk temperature, equation (5);
- λ, eigenvalue;
- $\boldsymbol{\Lambda}$, matrix of eigenvalues, equation (11);
- $\varphi, \boldsymbol{\varphi}$, dimensionless temperature gradient;
- ψ, solution of linear differential equation (10);
- ψ_0, ψ-vector at $z = 0$.

Subscript

- $+$, tube section $z > 0$;
- $-$, tube section $z < 0$.

1. INTRODUCTION

THE LINEAR partial differential equation (LPDE) is one of the most commonly encountered mathematical models for description of engineering systems. Standard examples of LPDE such as the linear heat equation in different geometries and with different boundary conditions are treated in several elementary textbooks. The standard techniques of solution employ the eigenfunctions of the differential operator, which form a "natural" basis for a series expansion of the solution of the LPDE. Quite often the associated boundary value problem is of the Sturm–Liouville type and the orthogonality of the eigenfunctions allows for a term by term calculation of the expansion coefficients A_k of the Fourier series. When the eigenfunctions are Bessel or circular functions explicit formulae for the eigenvalues and for A_k can be constructed and the solution of the LPDE can be written in a nice explicit form that permits a study of the effect of truncating the Fourier series after N terms. In case the eigenfunctions are less

simple or other complicating circumstances are present it is common practice to represent N eigenfunctions as accurately as possible by a numerical method and subsequently to use the tabular results in a numerical analogue of the procedure for trivial examples. Typically Hsu [1] determined the first 20 eigenvalues and the corresponding eigenfunctions by a Runge–Kutta technique in his recent study of the Graetz problem with axial conduction.

It is, however, by no means certain that the "classical Fourier series method" is the most practical numerical representation of the solution even when the Nth term can be written down explicitly. The trial functions of an N term approximation of the solution are chosen as the eigenfunctions of the differential operator without considering whether these are well suited for representation of the solution. This restrictive choice may lead to very slowly convergent series in practically important regions of the variables. Typical examples are the trigonometric functions that are eigenfunctions in many slab-symmetry problems. Villadsen and Sørensen [2] observed that polynomial trial functions represented the solution of the heat equation much better than trigonometric functions. The two dimensional steady state LPDE treated by Villadsen and Stewart [3] is even more typical. The Boussinesq double trigonometric series is very slowly convergent while a polynomial series converges within a few terms and is much better suited for tabulation of the solution.

The typical parabolic LPDE describes a transient phenomenon in terms of a generalized "time parameter" y. The Fourier series of exponentially damped eigenfunctions is theoretically best for large y, since for these y-values the true solution and the first term of the Fourier series become practically identical. For a finite y the classical eigenfunction expansion is not the optimal representation in any standard norm, and for small y the series is completely unsuited for numerical purposes.

When even an explicit expression for the truncated Fourier series may entail unnecessary computational work it appears irrational to imitate the behaviour of the truncated Fourier series by a numerical evaluation of the "true" eigenfunctions of the differential operator. The extra computational work involved in an individual treatment of each LPDE in a search for the true eigenfunctions is unlikely to be recompensated by an increased accuracy of the solution for any finite y-value.

The orthogonal collocation method operates with a fixed set of trial functions (Jacobi polynomials—often further restricted to Legendre polynomials), and the solution is found at discrete spatial values by a standardized interpolation scheme followed by an algebraic matrix–eigenvalue analysis. The small eigenvalues of the matrix are usually very close to the eigenvalues of the differential operator, but the large eigenvalues differ very much from the corresponding differential operator eigenvalues. This, however, does not by any means indicate that the resulting N-term approximation for the solution of the LPDE is inaccurate. On the contrary several papers by Finlayson [4], by Hlavaçek and coworkers (e.g. [5]) and by Villadsen and coworkers [2] have shown that extremely accurate results are obtained probably due to the superior quality of orthogonal polynomials as trial functions.

The purpose of the present paper is to give some explanation for this phenomenon, to indicate where specific advantages of the collocation method can be expected and on the basis of the Graetz problem with axial conduction, which is used here to illustrate the general collocation approach to LPDE, to suggest some interesting variants that could easily be solved by means of the same technique.

2. THE EXTENDED GRAETZ PROBLEM

A tube of radius R is insulated from $z = 0$ to $z \to -\infty$ and has a wall temperature of T_0 from $z = 0$ to $z \to \infty$. A Newtonian fluid is introduced at $z \to -\infty$ with temperature T_b. It flows in fully developed laminar flow through the tube and finally attains the temperature T_0 in the far downstream ($z \to \infty$) tube section. The model is the following linear partial differential equation

$$v_z \frac{\partial T}{\partial z} = 2\langle v_z \rangle \left(1 - \frac{r^2}{R^2}\right) \frac{\partial T}{\partial z} = \frac{k}{\rho c_p} \left(\frac{1}{r} \frac{\partial}{\partial r}\left(r \frac{\partial T}{\partial r}\right) + \frac{\partial^2 T}{\partial z^2}\right). \tag{1}$$

Suitable dimensionless variables are

$$x = \frac{r}{R}, \quad y = \frac{kz}{2\rho c_p \langle v_z \rangle R^2} = \frac{z}{PeR} \quad \text{and} \quad \theta = \frac{T - T_0}{T_b - T_0}$$

$$(1 - x^2) \frac{\partial \theta}{\partial y} = \frac{1}{x} \frac{\partial}{\partial x}\left(x \frac{\partial \theta}{\partial x}\right) + \frac{1}{Pe^2} \frac{\partial^2 \theta}{\partial y^2} \tag{2}$$

with

$$Pe = \frac{2R\langle v_z \rangle \rho c_p}{k}.$$

The boundary conditions of (2) are:

$$\theta = 1 \text{ for } y \to -\infty \text{ and } \frac{\partial \theta}{\partial x} = 0 \text{ for } x = 0. \tag{3}$$

$$\frac{\partial \theta}{\partial x} = 0 \text{ for } x = 1 \text{ and } y < 0;$$

$$\theta = 0 \text{ for } x = 1 \text{ and } y \geqslant 0.$$

In the standard treatment (e.g. [6] p. 295) of Graetz' problem equation (2) the last term is ignored, and this term is indeed of negligible importance when $Pe > 30$–50 except in an extremely small region $y \sim 0$ and close to the wall where the convective term is zero.

The eigenfunctions $F(x)$ of (2) are solutions of

$$\frac{1}{x}\frac{\mathrm{d}}{\mathrm{d}x}\left(x\frac{\mathrm{d}F}{\mathrm{d}x}\right)-\left((1-x^2)\lambda-\frac{\lambda^2}{Pe^2}\right)F=0. \qquad (4)$$

The boundary conditions of (4) are:

$$x=0: \quad \frac{\mathrm{d}F}{\mathrm{d}x}=0;$$

$$x=1: \quad \frac{\mathrm{d}F}{\mathrm{d}x}=0 \quad \text{for} \quad y<0$$

$$\text{and} \quad F=0 \quad \text{for} \quad y\geqslant 0.$$

The solution of (2) is:

$$\theta=\sum_0^\infty A_k F_k(x)\exp(\lambda_k y).$$

Since the boundary condition at $x=1$ is different for positive and for negative y separate sets of eigenvalues and eigenfunctions must be found for each region $y<0$ (λ_-, F_-) and $y>0$ (λ_+, F_+). Each set of eigenfunctions and eigenvalues must be found by numerical integration, e.g. by a Runge–Kutta method and adjustment of λ_k until

$$F_k(1)=0 \quad (y>0) \qquad \text{or} \qquad \left.\frac{\mathrm{d}F_k}{\mathrm{d}x}\right|_1=0 \quad (y<0).$$

Equation (4) is not a Sturm–Liouville problem for which F_k and F_j would be mutually orthogonal. Consequently the simple determination of the Fourier coefficients A_{k+} or A_{k-} fails. Hsu [1] expands both sets of eigenfunctions F_+ and F_- in sets of orthogonal functions f_+ and f_- by a Gram–Schmidt procedure and determines the coefficients of f_+ and f_- in the usual way. Finally the two separate solutions f_+ and f_- are spliced together at $y=0$. The whole numerical scheme is unnecessarily complicated especially since no increase in accuracy is expectable by using "true eigenfunctions". It is shown in a following section that the eigenfunction expansion is extremely slowly convergent for small Pe near $y=0$ and that Hsu's method due to insufficiency of the numerical process yields qualitatively erroneous results for small y.

It should briefly be mentioned that the numerical difficulties cannot be circumvented by relaxation of the boundary conditions (3) to $\theta=1$ at $y=0$ as attempted by Singh [7]. This is an indirect negation of the axial conduction contribution, which leads to a mathematically inconsequent problem formulation.

A number of derived quantities are used in the following:

(a) Bulk temperature $\bar{T}$ at distance z:

$$\int_A \rho c_p v_z T\,\mathrm{d}A=\bar{T}\int_A v_z \rho c_p\,\mathrm{d}A$$

or in terms of dimensionless temperature θ:

$$\bar{\theta}=\frac{\bar{T}-T_0}{T_b-T_0}=4\int_0^1 x(1-x^2)\theta\,\mathrm{d}x \qquad (5)$$

(b) $$Nu=\frac{2Rh}{k}=\frac{-2\left.\frac{\partial T}{\partial x}\right|_{x=1}}{\bar{T}-T_0}=-\frac{2\left.\frac{\partial\theta}{\partial x}\right|_{x=1}}{\bar{\theta}} \qquad (6)$$

(c) Total heat transfer to wall from $z=0$

$$J_z=\int_0^z -k\left.\frac{\partial T}{\partial r}\right|_{r=R}2\pi R\,\mathrm{d}z.$$

or

$$J=\frac{J_z}{J_\infty}=\frac{J_z}{\pi R^2\langle v_z\rangle\rho c_p(T_b-T_0)}=-4\int_0^y \left.\frac{\partial\theta}{\partial x}\right|_{x=1}\mathrm{d}y \qquad (7)$$

(d) For $Pe\to\infty$ $\bar{\theta}(y=0)=1$ and $J=1-\bar{\theta}$. (8)

3. NUMERICAL SOLUTION

The second order differential equation (2) is reformulated into two coupled first order equations:

$$\frac{\partial\theta}{\partial y}=\varphi$$

$$\frac{\partial\varphi}{\partial y}=\frac{\partial^2\theta}{\partial y^2}=Pe^2(1-x^2)\varphi-Pe^2\frac{1}{x}\frac{\partial}{\partial x}\left(x\frac{\partial\theta}{\partial x}\right) \qquad (2a)$$

The operator

$$\frac{1}{x}\frac{\partial}{\partial x}\left(x\frac{\partial\theta}{\partial x}\right)$$

is rewritten in terms of $u=x^2$:

$$\frac{1}{x}\frac{\partial}{\partial x}\left(x\frac{\partial\theta}{\partial x}\right)=4\left(u\frac{\partial^2\theta}{\partial u^2}+\frac{\partial\theta}{\partial u}\right).$$

Introducing $x^2=u$ and finding the solution which is finite at $u=0$ gives automatic satisfaction of the boundary condition $\partial\theta/\partial x=0$ at $x^2=u=0$.

The Nth order orthogonal collocation solution of (2a) is obtained when the residual of both equations is equated to zero at N values of u which are chosen as zeros u_i of an Nth degree orthogonal polynomial $P_N(u)$. In this paper the zeros of shifted Legendre polynomial have been chosen. The values of θ and of φ at u_i are respectively θ_i and φ_i. Each of the differential operators $\partial\theta/\partial u$ and $\partial^2\theta/\partial u^2$ is interpolated at each collocation point u_i by means of the collocation ordinate θ_j

$(j = 1, 2, \ldots, N)$ and the ordinate θ_{N+1} at $u = u_{N+1} = 1$:

$$u\frac{\partial^2\theta}{\partial u^2} \sim u_i \sum_{j=1}^{N+1} B_{ij}\theta_j$$

$$\frac{\partial\theta}{\partial u} \sim \sum_{j=1}^{N+1} A_{ij}\theta_j.$$

By this technique the coupled partial differential equations (2a) degenerate into $2N$ coupled ordinary differential equations

$$\begin{aligned}\frac{\mathrm{d}\theta}{\mathrm{d}y} &= \varphi \\ \frac{\mathrm{d}\varphi}{\mathrm{d}y} &= Pe^2\mathbf{V}\varphi - 4Pe^2(\mathbf{UB}+\mathbf{A})\theta.\end{aligned} \tag{9}$$

Here **A** and **B** are the collocation matrices for $\mathrm{d}\theta/\mathrm{d}u$ and for $\mathrm{d}^2\theta/\mathrm{d}u^2$.

U and **V** are diagonal matrices with respectively u_i and $1-u_i$ in the ith main diagonal position.

It is noted that matrices **A** and **B** are different in the two regions $y < 0$ and $y > 0$, since the formulas for the first and second derivatives both contain the wall value θ_{N+1}. This ordinate is zero for $y > 0$ but for $y < 0$ one must eliminate θ_{N+1} using the boundary condition

$$0 = \frac{\partial\theta}{\partial u} \sim \sum_{j=1}^{N+1} A_{N+1,j}\theta_j \qquad \text{for} \quad u = 1.$$

This elimination implies a correction of each of the remaining elements B_{ij} and A_{ij}, $(i,j) = (1, 2, \ldots, N)$.

Further details on the construction of **A** and **B** are given in [8].

The complete matrix formulation of (9) is

$$\frac{\mathrm{d}\boldsymbol{\psi}}{\mathrm{d}y} = \mathbf{Q}\boldsymbol{\psi}; \quad \boldsymbol{\psi} = (\theta_1, \theta_2, \ldots, \theta_N, \varphi_1, \varphi_2, \ldots, \varphi_N)^T$$

$$\mathbf{Q} = \begin{pmatrix} \mathbf{O} & \mathbf{I} \\ -4Pe^2(\mathbf{UB}+\mathbf{A}) & Pe^2\mathbf{V} \end{pmatrix} = \begin{cases} \mathbf{Q}_+ & \text{for } y \geqslant 0 \\ \mathbf{Q}_- & \text{for } y < 0. \end{cases} \tag{10}$$

Q is again different in the two y regions since **A** and **B** are different as explained above.

Equation (10) is solved by a standard matrix diagonalization technique:

$$\boldsymbol{\psi} = \begin{cases} \exp(\mathbf{Q}_+ y)\boldsymbol{\psi}_0 = \mathbf{S}_+ \exp(\mathbf{\Lambda}_+ y)\mathbf{S}_+^{-1}\boldsymbol{\psi}_0 \ (y \geqslant 0) & \text{(11a)} \\ \exp(\mathbf{Q}_- y)\boldsymbol{\psi}_0 = \mathbf{S}_- \exp(\mathbf{\Lambda}_- y)\mathbf{S}_-^{-1}\boldsymbol{\psi}_0 \ (y < 0). & \text{(11b)} \end{cases}$$

The diagonal matrices $\mathbf{\Lambda}_+$ and $\mathbf{\Lambda}_-$ contain the $2N$ eigenvalues of respectively $\mathbf{Q}_+$ and $\mathbf{Q}_-$. $\mathbf{Q}_+$ has N positive and N negative eigenvalues, $\mathbf{Q}_-$ has N positive and $N-1$ negative eigenvalues in addition to the eigenvalue 0, which is obtained for $y < 0$ due to the zero flux at the wall in this region.

From the boundary conditions ($\theta \to 0$ for $y \to \infty$ and $\theta \to 1$ for $y \to -\infty$) it is known that all collocation ordinates $\boldsymbol{\psi}_i$ must remain finite for $y \to \infty$ and for $y \to -\infty$.

Consequently the N positive exponentials which appear in (11a) for positive eigenvalues of $\mathbf{Q}_+$ and the $N-1$ positive exponentials which appear in (11b) for negative eigenvalues of $\mathbf{Q}_-$ must be suppressed by orthogonality relations between the eigenrows and the vector $\boldsymbol{\psi}_0$ of the dependent variable $\boldsymbol{\psi}$ at $y = 0$.

The rows of $\mathbf{S}_+^{-1}$ that correspond to positive eigenvalues of $\mathbf{Q}_+$ and the rows of $\mathbf{S}_-^{-1}$ that correspond to negative eigenvalues of $\mathbf{Q}_-$ must be orthogonal to $\boldsymbol{\psi}_0$. This yields $2N-1$ linear equations for the components of $\boldsymbol{\psi}_0$. The final $2N$th equation is obtained by the normalization $\theta_i \to 1$ for $y \to -\infty$, and all components of $\boldsymbol{\psi}_0$ can be found.

In summary the total solution $\boldsymbol{\theta}(y)$ is obtained by diagonalization of two $2N.2N$ matrices $\mathbf{Q}_+$ and $\mathbf{Q}_-$ and subsequent solution of $2N$ linear equations by Gauss elimination. The scalar quantity $\bar{\theta}(y)$ in (5) is directly obtained by Gauss quadrature using the $\boldsymbol{\theta}(y)$ values of (11).

4. QUALITATIVE BEHAVIOUR OF THE SOLUTION

The accuracy of the solution (11) to (2) is in principle determined by the success of the N-point interpolation applied in the x-direction, since the resulting set of ordinary differential equations (9) has a closed solution (11), which is accurate except for round-off errors in the QR algorithm used to determine the diagonalized form $\mathbf{SAS}^{-1}$ of **Q** and in the ensuing Gauss elimination routine for calculation of $\boldsymbol{\psi}_0$.

The magnitude of the negative eigenvalues λ_i of $\mathbf{Q}_+$ for $N = 12$ and $Pe \to \infty$ are compared in Table 1 with the eigenvalues of the differential operator in the classical Fourier series expansion. When $Pe \to \infty$ all positive eigenvalues of $\mathbf{Q}_-$ increase to infinity and the problem collapses into the ordinary Graetz problem

Table 1. Magnitudes of the eigenvalues for the classical Graetz problem ($Pe \to \infty$) compared with the collocation eigenvalues for $y > 0$ (negative eigenvalues of $\mathbf{Q}_+$ in (10)) for $N = 12$ collocation points

k	1	2	3	4	5	6	7	8	9	10	11	12
	Magnitudes of the eigenvalues											
Fourier series	7·318	44·61	113·9	215·2	348·5	513·9	711·2	940·5	1201	1495	1820	2178
Twelve point collocation	Difference between eigenvalues (Collocation–Fourier)						Magnitude of collocation eigenvalues					
	4.10^{-12}	5.10^{-11}	3.10^{-8}	2.10^{-4}	0·2	10·5	827·7	1539	3627	12243	81559	$4{\cdot}1.10^6$

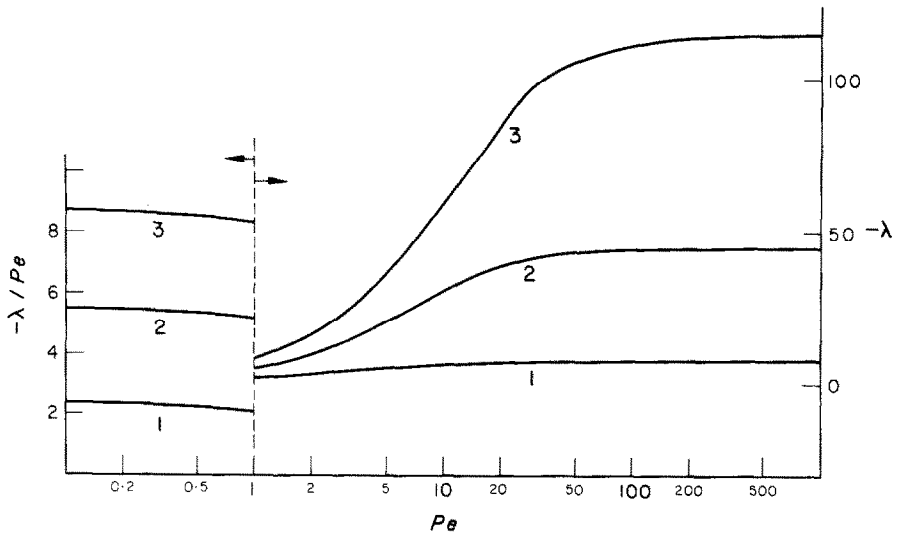

FIG. 1. First three negative eigenvalues of $\mathbf{Q}_+$ (equation 10) as function of Pe-number.

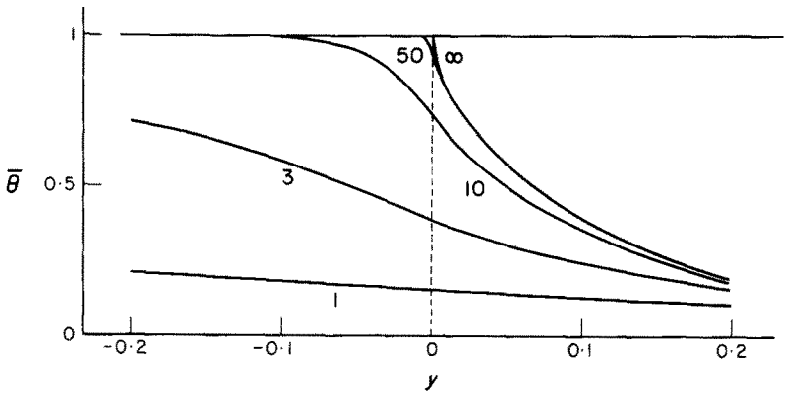

FIG. 2. Bulk mean temperature $\bar{\theta}$ defined by equation (5) as a function of axial position $y = z/RPe$ for discrete values of Pe.

with $\theta = 1$ at $y = 0$. The first two eigenvalues of $\mathbf{Q}_+$ are equal to the "Fourier eigenvalues" to within the accuracy of the QR algorithm. This means that the solution $\theta(y)$ or $\bar{\theta}(y)$ is identical to the Fourier series solution and hence to the exact solution for "large" y. This "far downstream" accuracy of the collocation solution was first observed by Villadsen and Stewart [3] for a specific LPDE, and has since then been discussed by Villadsen ([9] Chap. 1.7 and 3.1), by Finlayson ([10] Chap. 5) and by many others. It will not be further commented in this paper. Rather the attention of the next section will be focussed on the accuracy of the series solution in the region $y \sim 0$ where a comparison with boundary layer solutions will be made. The remainder of this section will be devoted to a qualitative discussion of the solution for finite Pe.

The first three negative eigenvalues of $\mathbf{Q}_+$ are shown in Fig. 1 as functions of Pe. For $Pe > 50$ they have practically the same values as in the limiting case $Pe \to \infty$.

Figure 2 shows that $\bar{\theta}(y)$ is also practically independent of Pe for $Pe > 50$ except in a small region close to $y = 0$. The gradient $\partial\bar{\theta}/\partial y$ is infinite at $y = 0$ for $Pe \to \infty$ and large but finite for $Pe = 50$. It rapidly approaches zero for negative y values. It is noted that a given $\bar{\theta}$-value is obtained at an axial position z/R which is proportional to Pe when $Pe \gtrsim 50$. Axial conduction is then negligible and Pe serves only as a scaling factor for axial distances.

In the Pe range $1 < Pe < 10$ $|\lambda_1|$, $|\lambda_2|$ and $|\lambda_3|$ rapidly decrease and diffusion into the upstream section is noticeable. For $Pe < 1$ the three eigenvalues become

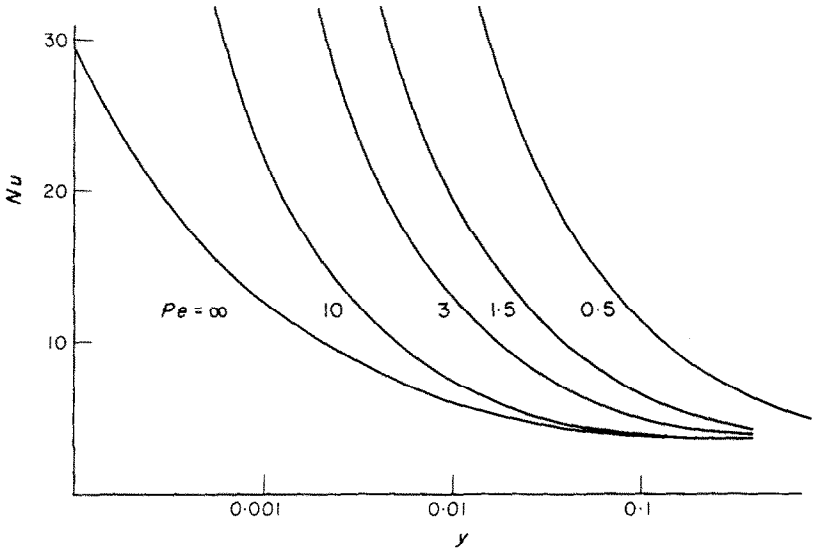

FIG. 3. Nusselt number defined by equation (6) as a function of y for discrete Pe-values.

proportional to Pe: $-\lambda_k = \rho_k Pe$, where ρ_k is the kth zero of $J_0(\rho)$ i.e. 2·40, 5·81 – (see Appendix, Section b2). The positive eigenvalues of $\mathbf{Q}_-$ also become proportional to Pe: $\lambda_k = \rho_k Pe$, where ρ_k is now the kth zero of $J_1(\rho)$.

The heat sink downstream from $y = 0$ will force θ to zero for every y when $Pe \to 0$. If, however, the Fourier coefficients and the eigenvalues are divided by Pe a well defined final solution for $Pe \to 0$ results. The behaviour of this solution for small z/R, which is the proper axial coordinate in this case, will be studied in Section 5.

Figure 3 shows $Nu(y)$ defined by (6) for various Pe-values. A similar figure is given by Hsu ([1] Fig. 3), but while Hsu's curves for $Nu(y)$ apparently approach a finite value for $y \to 0$ when $Pe < 10$ our curves show that $Nu \sim (yPe)^{-1/2}$ for $Pe < 10$ in much better agreement with some results of Newman [11] which are discussed in the next section. Thus the collocation exponential series must have much better convergence properties than the "true" Fourier series for small y even though the large eigenvalues of $\mathbf{Q}$ are blatantly different from the differential operator eigenvalues as exemplified in Table 1.

The far downstream behaviour of $Nu(y)$ is as expected identical by the two methods:

For $Pe \to \infty$ $Nu(y \gtrsim 1) \sim -\frac{1}{2}\lambda_1$ where λ_1 = the first negative eigenvalue of $\mathbf{Q}_+$, but as Pe decreases from infinity to zero the Nusselt number increases from 3·656 to 4·180 while $|\lambda_1|$ decreases from 7·31 to zero. A perturbation analysis which explains these results is given in Appendix A.

5. THE CHARACTER OF THE SOLUTION FOR SMALL y

Newman [12] has extended Leveque's similarity solution of (3) for $Pe \to \infty$ to the following three terms:

$$J(Pe \to \infty) = 1 - \bar{\theta} = 4{\cdot}0698y^{2/3} - 2{\cdot}4y - 0{\cdot}4454y^{4/3} + 0(y^{5/3}). \quad (12)$$

The first term represents J with an error less than 5 per cent for $y < 10^{-3}$.

Figure 4 shows J computed by 12 and 30 terms of the Fourier series (broken curves) compared with the solution by (12) and by a 12 point collocation solution (full curve). The truncated Fourier series is obviously not applicable for detection of the boundary-layer solution $J \sim 4{\cdot}0698y^{2/3}$ while the collocation series with $N = 12$ closely follows (12) at least down to $y = 10^{-5}$ where the first term of (12) is accurate to within 1 per cent. In the limit $y \to 0$ the collocation solution eventually breaks down, since the infinite slope

$$\left.\frac{\partial\theta}{\partial x}\right|_{x=1} \quad \text{for} \quad y = 0$$

cannot be represented by polynomials, but it does a much better job than the Fourier series for which convergence to J is found empirically to be

$$\ln(J(\text{Fourier}) - J(\text{true})) \sim \text{constant} \cdot N^{1/2}$$

where N is the number of terms in the series and the constant depends on y. More than 100 terms should be taken to obtain the same accuracy at $y = 2{\cdot}10^{-5}$ as the 12 point collocation solution.

The explanation is found in the rapid increase in magnitude of the eigenvalues λ_k of $\mathbf{Q}_+$ in Table 1. The

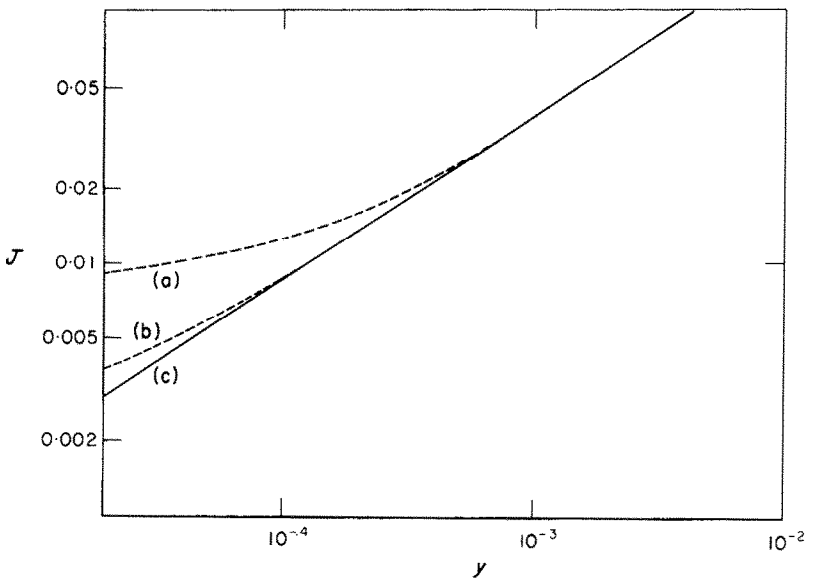

FIG. 4. Heat flux J defined by equation (7) as a function of y for $Pe \to \infty$. Curve (c): 12 point collocation and Newman's formula equation (12). Curves (a) and (b): Truncated Fourier series with twelve and thirty terms.

"Fourier eigenvalues" are approximately given by $-(4k-\frac{4}{3})^2$ [11] for $k > 7$–8, while the largest "collocation eigenvalue" is $-4{\cdot}16.10^6$ for $N = 12$. It is a prerequisite for an accurate eigenfunction series solution with a given number of terms N that $-\lambda_N y > 1$ and this is not satisfied for $y = 2{\cdot}10^{-5}$ by, e.g. a 12 term Fourier series. The expansion coefficients A_k decrease to zero with increasing k at about the same rate for the collocation series and for the Fourier series, but the much larger spread of collocation eigenvalues for $k > N/2$ makes the collocation series much faster convergent for small y. The large y convergence behaviour is fast and almost identical for the collocation series and for the true Fourier series due to the equivalence of the (A_k, λ_k) in the two series for small k.

It was noted in the previous section that the first three eigenvalues became proportional to Pe when $Pe \lesssim 1$. The same numerical relation is also obtained for larger Pe, but now only for the larger λ_k, since for increasing k the term λ_k^2/Pe^2 eventually dominates the factor of F in (4). Hence the large eigenvalues of (4) converge to $|\lambda_k| = Pek\pi$ since the large zeros of $J_0(\rho)$ and $J_1(\rho)$ occur with a distance of π. This means that the convergence of the Fourier series for small y becomes even more poor when Pe is finite, since the largest eigenvalue with N terms is proportional to N and not to N^2 as was the case for $Pe \to \infty$. An analysis of Hsu's eigenvalue data ([1] Table 1) shows that $\lambda_k (= -2\beta_k^2$ in the table$) = -Pe(\pi k - 1{\cdot}276)$ to within 0·005 per cent for $k > 4$ when $Pe = 1{\cdot}5$ and to within 2 per cent for $k > 9$ when $Pe = 3$. A similar analysis of the collocation eigenvalues for $N > 11$ shows that the largest negative eigenvalue of $\mathbf{Q}_+$ is represented by $\lambda_N = -1{\cdot}272Pe(N + 0{\cdot}5139)^2$ to within 0·002 per cent irrespective of the Pe value ($0{\cdot}2 < Pe < 300$). This almost schematic determination of λ_N is expectable, since $\mathbf{Q}_+$ has a fixed structure when the collocation points $\mathbf{u}$ and the order of approximation N has been chosen.

The main observation is again that the open-ended Fourier series consists of mutually independent terms which are determined one by one starting with the term that describes the far downstream behaviour of the solution, while the Nth order interpolative collocation scheme simultaneously determines the parameters of N orthogonal trial functions such that the remainder is incorporated also for finite y. This has no detrimental effect for large y since the first eigenfunctions are almost identical by the two methods, and at small y where the remainder of the N term Fourier series is large a very beneficial effect is noticed due to the better focusing power of the collocation series.

Figure 5 presents some numerical results obtained with $N = 17$ collocation points. The quantity J of formula (7), i.e. the total heat transfer to the tube wall from $y = 0$ to a given y value is studied as a function of y at discrete Pe values.

The circled points for $Pe = 0{\cdot}2$ show computed values similar to curve c on Fig. 4. A straight line portion of the curve can be found in the log–log plot

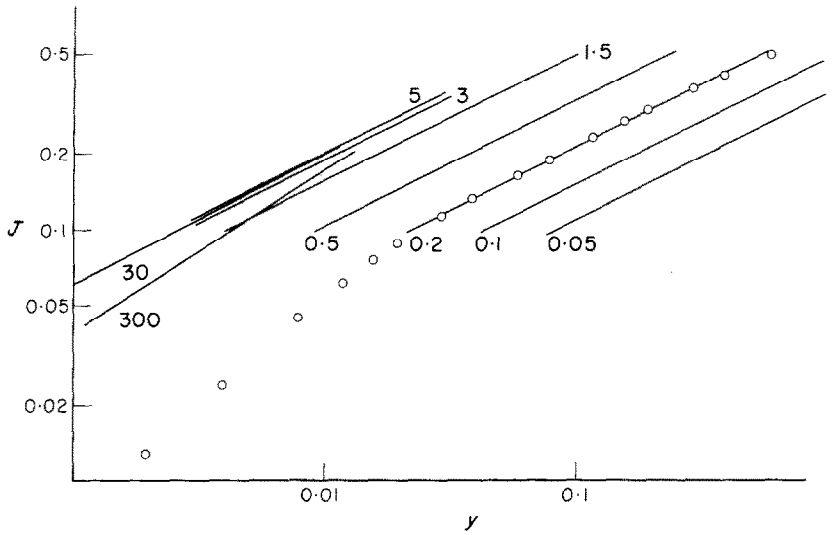

FIG. 5. J as a function of y for various values of Pe. The circled points indicate the range in which a seventeen point collocation solution fits the straight lines.

but while as a straight line is a valid representation of the collocation results in Fig. 4 at least to $y = 10^{-5}$ it will not be valid for $y < 0{\cdot}01$ even with 17 collocation points. This is due to the slow convergence of an exponential series representation of J for $y \sim 0$ especially for small Pe. Since a true Fourier series has a weaker convergence than the collocation series the true relationship $J \sim y^{1/2}$ for small y which is clearly observed on Fig. 5 could not have been found by means of a Fourier series.

For $J > 0{\cdot}5$ the straight line relationship does not either hold, in this case due to failure of a representation of the computed results for large J by the first term of a penetration theory series similar to (12) which only holds for $Pe \to \infty$.

The other lines on Fig. 5 are drawn through the straight line portions of curves computed for other Pe values using $N = 17$. The discussion for $Pe = 0{\cdot}2$ implies that the straight lines can be extended to $y = 0$, since the deviation of the computed results from the straight lines for small y is explained by a failure of the collocation solution.

Consequently the results on Fig. 5 can be used to deduct penetration theory results even though they are based on an expansion of the solution which is unsuitable for small y.

For $Pe < 0{\cdot}5$ it is seen that J is proportional to $(Pey)^{1/2}$ or $J = 1{\cdot}5(z/R)^{1/2}$ for $J < 0{\cdot}5$. It is expected that J is independent of Pe for $Pe \to 0$, since the convective term in (2) becomes insignificant in comparison with the axial diffusion term when $Pe \to 0$. The quantitative relationship which is found between J and z by an empirical analysis of the computer results is of some independent value and it could probably be confirmed by a technique similar to the one used by Levêque in the derivation of the first term of (12) for $Pe \to \infty$.

For $1{\cdot}5 < Pe < 3$ it is obvious that J is dependent on Pe as well as on z/R but the proportionality between J and $(z/R)^{1/2}$ still holds.

For $5 < Pe < 30$ practically the same curve is obtained which means that

$$J \propto y^{1/2} \quad \text{or} \quad J \propto (Pe^{-1/2})\left(\frac{z}{R}\right)^{1/2}.$$

For $Pe > 30$ the elliptical nature of the partial differential equation is discerned only in a very small region near $y = 0$ since the axial conduction term of (2) is negligible outside this region. Outside this region where $J \propto y^{1/2}$ the Levêque solution $J = 4{\cdot}07y^{2/3}$ of (12) holds until $y \sim 2{\cdot}10^{-3}$.

Newman [11] first detected the $J \propto y^{1/2}$ solution behind the Levêque solution for large but finite Pe by using a singular perturbation technique inwards from the Levêque solution. It is obvious that his result $J = 4{\cdot}24Pe^{-1/4}y^{1/2}$ for $y \lesssim 10^{-5}$ behind the Levêque solution is extremely difficult to detect by an analysis of numerical data based on an exponentially decreasing series and only the "Levêque" portion of the results are shown on Fig. 5 for $Pe = 300$.

6. SUGGESTIONS FOR FURTHER WORK

The previously published examples of solutions of linear partial differential equation (LPDE) and the more general observations based on the eigenvalue spectrum made in the present paper suggest that the

solution of these mathematical models by a combination of orthogonal collocation and matrix methods can give results of equal applicability for large and for small values of the unrestricted independent variable. This means that the similarity or singular perturbation solutions, which are often quite hard to develop by semi-analytical methods, can be avoided at least for qualitative studies of the solution.

The matrix methods of Section 3 are quite generally applicable for any LPDE and also for non-linear equations if they are coupled to an iterative process, e.g. a Newton–Raphson method. An interesting variant of the collocation method, the so-called spline-collocation [13], can be used to improve the accuracy for small y. The profile $\theta(y)$ is very steep near $x = 1$ for small y and a global approximation of $\theta(x)$ by polynomials is not accurate—the results on Fig. 5 for $N = 17$ illustrate the failure of the method for small y. If on the other hand the x interval $[0, 1]$ is split into two subintervals of which one extends from $x = 1$ to x_s where x_s may be, e.g. 0·8 one may apply collocation to each interval, splicing the two parts of the profile together at x_s by demanding continuity of θ and $\partial\theta/\partial x$. Preliminary investigations on this example show that a total of 7 collocation points of which 3 are allocated to the small interval $(x_s, 1)$ and 4 to $(0, x_s)$ gives the same accuracy as a global method with $N = 12$. Further applications of this method which may be very useful in many examples with steep profiles are given in [13].

Heat transfer to pseudo-plastic materials in tubes

$$\left(v_z = \left(1 + \frac{2}{M}\right)\langle v_z\rangle(1 - x^M) \quad \text{with} \quad M > 2\right)$$

may constitute an interesting example where axial conduction plays a significant role. Brinkman's problem of viscous heating of fluids flowing in small bore tubes under large pressure gradients is another example where preliminary calculations show that axial conduction has an appreciable effect. Both examples are solved by an exact repetition of the algorithms in Section 3.

REFERENCES

1. C. W. Tan and C. J. Hsu, Low Peclet number mass transfer in laminar flows through circular tubes, *Int. J. Heat Mass Transfer* **15**, 2187–2201 (1972).
2. J. Villadsen and J. P. Sørensen, Solution of parabolic partial differential equations by a double collocation method, *Chem. Engng Sci.* **24**, 1337–1349 (1969).
3. J. Villadsen and W. E. Stewart, Solution of boundary-value problems by orthogonal collocation, *Chem. Engng Sci.* **22**, 1483–1501 (1967).
4. B. Finlayson, Packed bed reactor analysis by orthogonal collocation, *Chem. Engng Sci.* **26**, 1081–1091 (1971).
5. V. Hlavaçek and M. Kubicek, Qualitative analysis of the behaviour of nonlinear parabolic equations, *Chem. Engng Sci.* **26**, 1737–1752 (1971).
6. R. B. Bird, W. E. Stewart and E. Lightfoot, *Transport Phenomena*. Wiley, New York (1960).
7. S. N. Singh, Heat transfer by laminar flow in a cylindrical tube, *Appl. Scient. Res.* **A7**, 325–340 (1958).
8. M. L. Michelsen and J. Villadsen, A convenient computational procedure for collocation constants, *Chem. Engr Jl* **4**, 64–68 (1972).
9. J. Villadsen, Selected approximation methods for chemical engineering problems, Instituttet for Kemiteknik, DtH, Lyngby (1970).
10. B. Finlayson, *The Method of Weighted Residuals and Variational Principles*. Academic Press, New York (1972).
11. J. Newman, The Graetz problem, UCRL-report No. 18646 (1969).
12. J. Newman, Extension of the Levêque solution, *J. Heat Transfer* **91**, 177–181 (1969).
13. J. Villadsen, Applications of the collocation method, Instituttet for Kemiteknik (1972). (Available on request.)

APPENDIX A

In this appendix a perturbation solution of equation (4) is developed. The main results are formulae (9A) and (12A) for the far downstream Nusselt number Nu_{as} when the Peclet number is large or small. The numerical value of Nu_{as} can easily be obtained with a low order collocation method and in this respect nothing new is offered. It is on the other hand a temptation to develop semi-analytical explanations for the numerical behaviour of the solution, which is known with many digits accuracy from the collocation method—in fact this "development of formulae by hindsight" is probably the most valuable feature of any accurate numerical method.

Formulae (5A) and (6A) that represent the general results of the perturbation method have a wide applicability for approximate solution of any boundary value problem, which is formulated as a perturbation to a Sturm–Liouville problem.

(a) *General treatment*

Let a Sturm–Liouville equation be perturbed by $\alpha f(x, \lambda)F$ where α is a small constant and $f(x, \lambda)$ is a specified function of x and λ

$$\frac{\mathrm{d}}{\mathrm{d}x}\left(p(x)\frac{\mathrm{d}F}{\mathrm{d}x}\right) + (q(x) + \lambda r(x))F + \alpha f(x, \lambda)F = 0. \quad (1A)$$

It is desired to find the first eigenvalue λ and the corresponding eigenfunction $F(x)$ as perturbations to the first eigenvalue λ_1 and eigenfunction $F_1(x)$ of the simplified problem with $\alpha = 0$.

$$\lambda = \lambda_1 + \alpha\lambda^* \quad \text{and} \quad F = F_1 + \alpha F^*. \quad (2A)$$

The whole set of eigenvalues and eigenfunctions $\{\lambda_i, F_i(x)\}$ of the unperturbed problem is assumed to be known. Equation (2A) is inserted into (1A) and terms in $\alpha^2, \ldots,$ are discarded.

$$\frac{\mathrm{d}}{\mathrm{d}x}\left(p(x)\frac{\mathrm{d}F^*}{\mathrm{d}x}\right) + \lambda^* F_1 r(x) + (q(x) + \lambda_1 r(x))F^* + f(x, \lambda_1)F_1 = 0 \quad (3A)$$

F^* is expanded in a Fourier series on the set $\{F_i\}$ $i = 2, \ldots,$ and inserted into (3A)

$$F^* = \sum_2^\infty c_i F_i(x)$$

and

$$\frac{\mathrm{d}}{\mathrm{d}x}\left(p(x)\frac{\mathrm{d}F^*}{\mathrm{d}x}\right) = -\sum_2^\infty c_i(q(x)+\lambda_i r(x))F_i$$

$$\lambda^* F_1 r(x) + \sum_2^\infty c_i(\lambda_1-\lambda_i)r(x)F_i + f(x,\lambda_1)F_1 = 0 \qquad (4A)$$

λ^* and c_j are found from (4A) by multiplication with respectively F_1 and F_j followed by integration over the orthogonality interval (a, b)

$$\lambda^* \int_a^b r(x)F_1^2\,\mathrm{d}x = -\int_a^b f(x,\lambda_1)F_1^2\,\mathrm{d}x \qquad (5A)$$

$$c_j(\lambda_1-\lambda_j)\int_a^b r(x)F_j^2\,\mathrm{d}x = -\int_a^b f(x,\lambda_1)F_1F_j\,\mathrm{d}x. \qquad (6A)$$

Since all integrals in (5A) and (6A) can be found either analytically or by quadrature these equations provide explicit values for λ^* and c_j.

(b) *Application of* (5A) *and* (6A) *to the extended Graetz problem*

(1) *Large values of Pe.*

$$\frac{\mathrm{d}}{\mathrm{d}x}\left(x\frac{\mathrm{d}F}{\mathrm{d}x}\right) - \lambda(1-x^2)xF + \frac{\lambda^2}{Pe^2}xF = 0. \quad \text{(7A and 4)}$$

In the notation of (3A):

$$r(x) = -x(1-x^2), \quad \alpha = \frac{1}{Pe^2} \quad \text{and} \quad f(x,\lambda_1) = x\lambda_1^2.$$

The eigenfunctions $\{F_i\}$ of (7A) with $\alpha = 0$ are Graetz' functions and the eigenvalues for $y > 0$ are

$$\{\lambda_i\} = -7{\cdot}3135869,\ -44{\cdot}60946, \ldots,$$

$$\lambda^* = \int_0^1 \lambda_1^2 xF_1^2\,\mathrm{d}x \Big/ \int_0^1 x(1-x^2)F_1^2\,\mathrm{d}x$$
$$= 1{\cdot}251225\lambda_1^2 = 66{\cdot}926.$$

The integrals can either be determined from the power series for F_1 or by Gaussian quadrature using the collocation ordinates $\theta(y)$ for $y \gtrsim 1$ and $Pe \to \infty$.

Hence the first eigenvalue of (4) is

$$\lambda \cong \lambda_1 + \frac{66{\cdot}926}{Pe^2} = -7{\cdot}3135869 + \frac{66{\cdot}926}{Pe^2}. \qquad (8A)$$

The asymptotic Nusselt number for large Pe is obtained by integration of (7A) with F = first eigenfunction

$$-\left.\frac{\mathrm{d}F}{\mathrm{d}x}\right|_{x=1} = \frac{\lambda^2}{Pe^2}\int_0^1 xF\,\mathrm{d}x - \lambda\int_0^1 x(1-x^2)F\,\mathrm{d}x$$

$$Nu_{as} = \frac{-2\left.\frac{\mathrm{d}F}{\mathrm{d}x}\right|_{x=1}}{\bar{F}}$$

$$= \frac{2\left(\frac{\lambda^2}{Pe^2}\int_0^1 xF\,\mathrm{d}x - \lambda\int_0^1 x(1-x^2)F\,\mathrm{d}x\right)}{4\int_0^1 x(1-x^2)F\,\mathrm{d}x}$$

$$= -\frac{\lambda}{2} + \frac{\lambda^2}{2Pe^2}\int_0^1 xF\,\mathrm{d}x \Big/ \int_0^1 x(1-x^2)F\,\mathrm{d}x$$

$$\sim -\frac{\lambda_1}{2} + \frac{1}{Pe^2}\left(-\frac{\lambda^*}{2} + \frac{\lambda_1^2}{2}\int_0^1 xF_1\,\mathrm{d}x \Big/ \int_0^1 x(1-x^2)F_1\,\mathrm{d}x\right)$$

$$= -\frac{\lambda_1}{2} + \frac{4{\cdot}487}{Pe^2} \qquad (9A)$$

Table 2 shows that λ as well as Nu_{as} are determined with a high accuracy for $Pe > 30$ and that the perturbation formulae give a tolerable accuracy even at $Pe = 5$. Note that the approximation $Nu_{as} = -\frac{1}{2}\lambda$ which holds for a true Sturm–Liouville problem is qualitatively in error, since the perturbation of the first eigenfunction (last term in 9A) is larger than the perturbation λ^*/Pe^2 of λ_1.

Table 2. The first eigenvalue for $y > 0$ and the asymptotic Nu-number for large Pe by collocation and by perturbation (8A, 9A)

Pe	100	30	10	5
$-\lambda$ (17 point colloc.)	7·3069064	7·2406920	6·744049	5·68967
$-\lambda$ by (8A)	7·306894	7·23922	6·6436	4·63
Relative difference	$1{\cdot}7.10^{-6}$	$2{\cdot}0.10^{-4}$	$1{\cdot}3.10^{-2}$	0·14
Nu (17 point colloc.)	3·6572414	3·66168	3·69518	3·7672
Nu by (9A)	3·6572421	3·66178	3·70166	3·8363
Relative difference	$< 10^{-6}$	$2{\cdot}5.10^{-5}$	$1{\cdot}8.10^{-3}$	2.10^{-2}

(2) *Small values of Pe.* Equation (4) is rescaled by taking an axial coordinate $y = z/R$:

$$\frac{\mathrm{d}}{\mathrm{d}x}\left(x\frac{\mathrm{d}F}{\mathrm{d}x}\right) + \lambda^2 xF - \lambda Pex(1-x^2)F = 0$$
$$r(x) = x, \quad \alpha = Pe, \quad \text{and} \quad f(x,\lambda_1) = -\lambda_1 x(1-x^2). \qquad (10A)$$

The eigenfunctions $\{F_i\}$ of (10A) with $\alpha = 0$ are Bessel functions $J_0(\lambda_i x)$ where λ_i are the negative zeros of $J_0(\rho)$, $\lambda_1 = -2{\cdot}4048256$, $\lambda_2 = -5{\cdot}52$ etc. and $\lambda^2 = (\lambda_1 + \alpha\lambda^*)^2 \sim \lambda_1^2 + 2\alpha\lambda_1\lambda^*$.

Consequently the development from (2A) to (5A) yields

$$\lambda^* = \tfrac{1}{2}\int_0^1 x(1-x^2)J_0^2(\lambda_1 x)\,\mathrm{d}x \Big/ \int_0^1 xJ_0^2(\lambda_1 x)\,\mathrm{d}x = 0{\cdot}39095$$

$$\lambda = -2{\cdot}4048256 + 0{\cdot}39095\,Pe. \qquad (11A)$$

The coefficients c_j of (6A) are

$$c_j = \frac{1}{\lambda_1^2-\lambda_j^2}\frac{\int_0^1 \lambda_1 x(1-x^2)J_0(\lambda_1 x)J_0(\lambda_j x)\,dx}{\int_0^1 xJ_0^2(\lambda_j x)\,dx} = \frac{2\lambda_1}{J_1^2(\lambda_j)(\lambda_1^2-\lambda_j^2)}\int_0^1 x(1-x^2)J_0(\lambda_1 x)J_0(\lambda_j x)\,dx.$$

The first four c_j are found by numerical quadrature:

$$10^2\{c_j\} = \{2{\cdot}5895,\ -0{\cdot}2320,\ 0{\cdot}0515,\ -0{\cdot}0170\}$$

Nu_{as} is obtained in the same way as for large Pe:

$$-\left.\frac{dF}{dx}\right|_{x=1} = \int_0^1 \lambda^2 xF\,dx - \lambda\int_0^1 Pex(1-x^2)F\,dx$$

$$Nu_{as} = -\frac{Pe\lambda}{2}+\frac{\lambda^2}{2}\int_0^1 xF\,dx\Big/\int_0^1 x(1-x^2)F\,dx$$

$$\sim -\frac{Pe\lambda}{2}+\frac{\lambda_1^2+2\lambda_1\lambda^*Pe}{2}\frac{\int_0^1 xJ_0(\lambda_1 x)\,dx+Pe\sum_2^\infty c_j\int_0^1 xJ_0(\lambda_j x)\,dx}{\int_0^1 x(1-x^2)J_0(\lambda_1 x)\,dx+Pe\sum_2^\infty c_j\int_0^1 x(1-x^2)J_0(\lambda_j x)\,dx}$$

$$= -\frac{Pe\lambda}{2}+\frac{\lambda_1^2+2\lambda_1\lambda^*Pe}{2}\frac{I_1+PeS_1}{I_2+PeS_2}$$

$$\sim \frac{\lambda_1^2}{2}\frac{I_1}{I_2}+Pe\left(-\frac{\lambda_1}{2}+\frac{\lambda_1\lambda^*I_1}{I_2}+\frac{\lambda_1^2}{2}\left(\frac{S_1}{I_2}-\frac{S_2I_1}{I^2}\right)\right)$$

$$I_{1j} = \int_0^1 xJ_0(\lambda_j x)\,dx = \frac{J_1(\lambda_j)}{\lambda_j}$$

$$I_{2j} = \int_0^1 x(1-x^2)J_0(\lambda_j x)\,dx = \frac{4}{\lambda_1^3}J_1(\lambda_j)$$

$$S_1 = -0{\cdot}16815.10^{-2} \quad \text{and} \quad S_2 = -0{\cdot}02137.10^{-2}$$

Hence the value of Nu_{as} for $Pe = 0$ is

$$\frac{\lambda_1^2}{2}\frac{I_1}{I_2} = \frac{\lambda_1^4}{8} = 4{\cdot}180654$$

and the perturbation formula is

$$Nu \sim 4{\cdot}180654 + Pe(1{\cdot}202412 - 1{\cdot}359292 - 2{\cdot}6580.10^{-2}) = 4{\cdot}180654 - 0{\cdot}1835Pe. \tag{12A}$$

The perturbation is again seen to result as a small difference between larger terms, and the inclusion of several terms of the perturbed eigenfunction is necessary. The accuracy of (11A) and (12A) is from Table 3 seen to be very satisfactory for $Pe < 1$ and acceptable up to $Pe \sim 1{\cdot}5$.

Table 3. The first eigenvalue for $y > 0$ and Nu_{as} for small Pe by collocation and by perturbation (11A, 12A). Note: Eigenvalues of this table are the eigenvalues of (4) divided by Pe

Pe	0·05	0·2	0·5	1	1·5
$-\lambda$ (17 point colloc.)	2·38535	2·32784	2·21695	2·04437	1·8869
$-\lambda$ by (11A)	2·38527	2·32663	2·20935	2·014	1·62
Relative difference	$3{\cdot}3.10^{-5}$	$5{\cdot}2.10^{-4}$	$3{\cdot}4.10^{-3}$	$1{\cdot}5.10^{-2}$	0·13
Nu (17 point colloc.)	4·171561	—	4·09685	4·02735	3·96985
Nu by (12A)	4·171479	4·14395	4·08890	3·997	3·905
Relative difference	$1{\cdot}9.10^{-5}$	—	$1{\cdot}9.10^{-3}$	$7{\cdot}5.10^{-3}$	$1{\cdot}6.10^{-2}$

LE PROBLEME DE GRAETZ AVEC CONDUCTION THERMIQUE AXIALE

Résumé—Le problème de Graetz avec conduction thermique axiale est traité comme illustration d'une méthode de résolution d'une classe très importante d'équations linéaires aux dérivées partielles. La méthode est une combinaison de la collocation orthogonale et de la diagonalisation de matrice. La raison de la très grande précision, obtenue par collocation, est discutée à partir des valeurs propres de l'opérateur de collocation. On trouve qu'elles croissent plus vite que les valeurs propres vraies pour $k > N/2$, où N est le nombre de points de collocation et ceci permet aussi une grande précision dans la "région de pénétration" de la solution où les séries de Fourier sont lentement convergentes.

On développe en appendice des formules explicites donnant le nombre de Nusselt asymptotique pour un nombre de Péclet soit grand, soit petit. Elles sont basées sur une perturbation des fonctions propres du modèle simplifié, avec un nombre de Péclet infini ou nul.

On propose des variantes du problème de Graetz qui peuvent être résolues par une répétition des calculs présentés.

DAS GRAETZ-PROBLEM MIT AXIALER WÄRMELEITUNG

Zusammenfassung—Am Beispiel des Graetz-Problems mit axialer Wärmeleitung wird ein Lösungsverfahren für eine wichtige Klasse linearer partieller Differentialgleichungen entwickelt. Die Methode ist eine Kombination aus orthogonaler Kollokation und Matrix-Diagonalisierung. Der Grund für die durch die Kollokation erreichte sehr hohe Genauigkeit wird anhand der Eigenwerte des Kollokations-Operators diskutiert. Es zeigt sich, daß diese viel schneller anwachsen als die wahren Eigenwerte für $k > N/2$—mit N als der Anzahl der Kollokations-Punkte; dies erlaubt eine hohe Genauigkeit auch in der "Durchdringungsregion" der Lösung, in der Fourier-Reihen langsam konvergieren.

Explizite Ausdrücke für die asymptotische *Nu*-Zahl für große und kleine *Pe*-Zahlen werden in einem Anhang aufgestellt. Sie basieren auf einer Störung der Eigenwerte des vereinfachten Modells mit unendlich großen oder sehr kleinen *Pe*-Zahlen. Weiter werden einige Varianten des Graetz-Problems, die durch eine Wiederholung der vorliegenden Berechnungen gelöst werden können, vorgeschlagen.

ЗАДАЧА ГРЕТЦА ПРИ ОСЕВОЙ ТЕПЛОПРОВОДНОСТИ

Аннотация — Используя задачу Гретца при осевой теплопроводности в качестве примера, разработан метод решения важного класса линейных дифференциальных уравнений в частных производных. Метод представляет собой комбинацию ортогональных коллокаций и матричной диагонализации. Высокая точность, полученная путем коллокаций, объясняется с помощью собственных значений оператора коллокаций. Найдено, что собственные значения оператора коллокаций увеличиваются гораздо быстрее, чем истинные собственные значения при $K > N/2$, где N — число точек коллокаций, что также приводит к большой точности в «области проникновения» решения, в которой медленно сходится ряд Фурье.

В приложении получены формулы в явном виде для асимптотического числа Нуссельта при больших и малых числах Пекле. Они основаны на возмущении собственных функций упрощенной модели при бесконечном или нулевом числе Пекле.

Предлагается несколько вариантов задачи Гретца, которые можно решить путем повторения настоящих расчетов.